Biodegradable Nanogel Formation of Polylactide-Grafted Dextran Copolymer in Dilute Aqueous Solution and Enhancement of Its Stability by Stereocomplexation

Koji Nagahama, Yousuke Mori, Yuichi Ohya,* and Tatsuro Ouchi*

Department of Applied Chemistry, Faculty of Engineering and High Technology Research Center, Kansai University, Suita, Osaka 564-8680, Japan

Received February 20, 2007; Revised Manuscript Received April 21, 2007

Monodisperse stereocomplex nanogels were obtained through the self-assembly of an equimolar mixture of dextran-*graft*-poly(L-lactide) (Dex-*g*-PLLA) and dextran-*graft*-poly(D-lactide) (Dex-*g*-PDLA) amphiphilic copolymers with well-defined composition in a dilute aqueous solution. The stereocomplex nanogel possessed partially crystallized cores of hydrophobic polylactide (PLA) and the hydrophilic dextran skeleton by intra- and/or intermolecular self-assembly between PLLA and PDLA chains. The stereocomplex nanogels exhibited significantly lower critical aggregation concentration (CAC) value as well as stronger thermodynamic stability compared with those of the corresponding L- or D-isomer nanogels. The mean diameter of the stereocomplex nanogels was 70 nm with narrow size distribution, implying they were well-defined and presumably nanogels. Furthermore, stereocomplex nanogel exhibited strong kinetic stability. The tunable degradation properties of Dex-*g*-PLA nanogels were achieved by varying the number of grafted PLA chains as well as applying stereocomplexation. This study demonstrates the advantage of stereocomplexation in the design of biodegradable nanogels with enhanced stability.

Introduction

Amphiphilic molecules self-assemble into various structures such as spherical and cylindrical nanometric particles, lamellae, and vesicles in aqueous media.[1−3] Those self-assemblies have been extensively studied for past decade due to their unique characteristics and the variety of application in many areas, including the biomedical field. In particular, the spherical nanometric particles made of graft copolymers with high molecular weight of hydrophilic main chain and short hydrophobic side chains, known as nanogels, have been paid a great deal of recent attention with their high potential use as artificial molecular chaperones and vehicles for delivery of hydrophilic bioactive agents as well as hydrophobic compounds.[4−10] The efficiency of these molecules as therapeutic agents may be related to many factors, including the ability of vehicles to cross biological barriers, to reach the target site, and to release the encapsulated molecules gradually. Additionally, bioactive agents such as proteins, peptides, and genes are very unstable compounds that need to be protected from degradation in the biological environment. So, the stability of vehicles is also a key factor to determine the efficiency of these bioactive molecules as therapeutic agents. Therefore, the biodegradable nanogels with strong stability exhibit great advantages for requirements such as long circulation times, accumulation at targeted sites, and controlled drug release as the vehicles of bioactive agents.

Strategies to yield drug vehicles to improved stability rely mostly on chemical cross-linking.[11,12] On the other hand, when the stability of drug vehicles is improved for delivery of bioactive agent, cross-linking by physical interactions has several advantages over chemical cross-linking, because it avoids the use of photoirradiation, organic solvents, auxiliary cross-linking agents, and/or other reactive molecules that may damage bioactive agents to be incorporated.

Polylactide (PLA) is a biodegradable and biocompatible polymer that is widely used in the biomedical field.[13−15] PLA synthesized from enantiomeric L- and D-lactic acids are poly(L-lactide) (PLLA) and poly(D-lactide) (PDLA), respectively. PLLA and PDLA, similar to other chiral polymers, can form a racemate, the physical properties of which are different from those of the individual enantiomers. The racemate of chiral polymers were called stereocomplexes although the formation of a racemate has nothing to do with complexation in its original sense. Such a stereocomplex displays a melting point 50 °C above that of the individual enantiomers. Interestingly, stereocomplexes are characterized by higher physical and chemical stabilities.[16−18] Stereocomplexation of PLA was induced recently exploited to trigger gel formation in water of amphiphilic copolymers for the design of sustained release devices.[19−24]

Some research groups have reported the synthesis of PLA-grafted dextran copolymers and evaluation of their possibility as biomedical materials.[25−27] On the other hand, we previously reported the synthesis of water-insoluble amphiphilic PLLA-grafted dextran copolymers (Dex-*g*-PLLA) and the physicochemical properties as well as protein adsorption and cell attachment behaviors of its solution cast film.[28,29] In this article, we synthesized water-soluble biodegradable graft copolymers of Dex-*g*-PLLA and Dex-*g*-PDLA and investigated their ability to form nanometric aggregates in an aqueous solution. We report here the preliminary results showing that it is indeed possible to obtain nanogels from the enantiomeric Dex-*g*-PLLA and Dex-*g*-PDLA copolymers by intra- and/or intermolecular self-assembly of PLA chains in a dilute aqueous solution. Furthermore, by simply mixing the aqueous solutions of the enantiomeric Dex-*g*-PLLA and Dex-*g*-PDLA, we succeeded in stabilization of the nanogels because the cores of PLA-based nanogels could crystallize in a stereocomplex configuration.

* Corresponding authors: tel +81-6-6368-0814; fax +81-6-6330-4026; e-mail touchi@ipcku.kansai-u.ac.jp (T.O.) or yohya@ipcku.kansai-u.ac.jp (Y.O.).

10.1021/bm070206t CCC: $37.00
Published on Web 06/09/2007

Scheme 1. Synthesis of Dex-*g*-PLLA and Dex-*g*-PDLA Copolymers

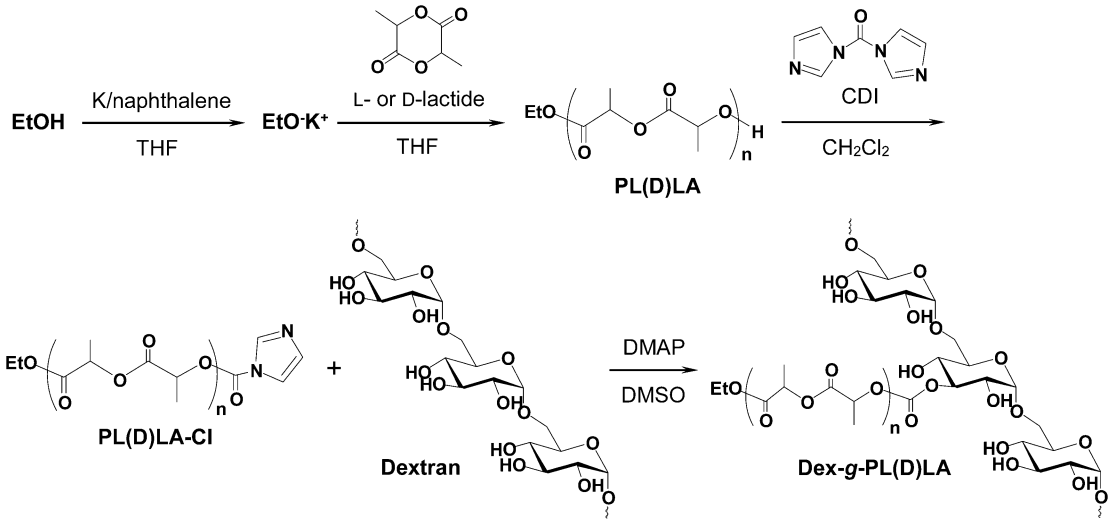

Experimental Section

Materials. L-Lactide and D-lactide were purchased from Purac Biochem BV (Gorinchem, The Netherlands) and used without further treatment. Dextran (M_n = 40 000, M_w/M_n = 1.7) was purchased from Sigma Chemical Co. (St. Louis, MO) and dried at 60 °C in vacuo before use. Ethanol, naphthalene, dry tetrahydrofuran (THF), dry dimethyl sulfoxide (DMSO), *N*,*N*′-carbonyldiimidazole (CDI), 4-(*N*,*N*-dimethylamino)pyridine (DMAP), and sodium dodecyl sulfate (SDS) purchased from Wako Pure Chemical Co. were used as received. All other chemicals were reagent-grade and were used without further purification.

Synthesis of Enantiomeric PLLA and PDLA. Mono-hydroxyl-terminated PLLA and PDLA were synthesized by ring-opening polymerization of L- AND D-lactide with ethanol as an initiator, as shown in Scheme 1. The following anionic polymerization was carried out in a glove box purged with dry argon. A hydroxyl end group of ethanol was transformed to the potassium alkoxide end group with potassium (K)/naphthalene in dry THF. Naphthalene (1.96 g; 15.3 mmol) and a small amount of potassium were added to dry THF (7.7 mL) and then stirred to obtain a THF solution of K/naphthalene (deep green), which was added to a THF solution (5.0 mL) of ethanol (180 μL; 5.1 mmol), and the resulting mixture was stirred for 60 min to prepare the potassium alkolate of ethanol, potassium ethoxide. L- OR D-Lactide (8.81 g; 61.2 mmol) in THF solution (30.6 mL) was added to the resulting potassium ethoxide solution. After 15 min, the polymerization of L- OR D-lactide was terminated by addition of 517 μL of acetic acid (10.2 mmol) to the reaction mixture. The obtained product was precipitated in diethyl ether and dried under vacuum overnight to yield the white solid of mono-hydroxyl-terminated PLLA or PDLA with DP 20. Relative number-average molecular weight ($M_{n,GPC}$) and molecular weight distribution (M_w/M_n) of the synthesized PLAs was estimated by gel-permeation chromatography [GPC; Tosoh GPC-8020 series system (column, TSK-Gel Alpha-5000 × 2; eluent, DMF; detector, refractive index; standard, PS)]. Number-average molecular weight ($M_{n,NMR}$) and the degree of polymerization (DP) were estimated by ^{1}H NMR spectroscopy [JEOL GSX-400, internal reference TMS]. The specific optical rotation ([α]) of the obtained PLLA and PDLA were measured in chloroform at a concentration of 10 mg/mL and 25 °C ($[\alpha]_D^{25}$) on a polarimeter (Horiba SEPA-300) at a wavelength of 589 nm.

Synthesis of Activated PLLA and PDLA. To couple the PLA to dextran, the hydroxyl group of the PLA was activated by use of CDI.[19] In brief, CDI (1070 mg; 6.2 mmol) was dissolved in dry chloroform (5 mL) in a nitrogen atmosphere. PLLA-OH or PDLA-OH (7000 mg; 2.5 mmol) was dissolved in chloroform (7 mL) and added to the CDI solution. The reaction mixture was stirred for 6 h at room temperature in a nitrogen atmosphere. Thereafter, the reaction mixture was washed with a large amount of ethanol to remove the excess CDI and imidazole. The obtained precipitate was collected by centrifugation and dried under vacuum overnight to yield the white solid of PLLA-CI or PDLA-CI with DP 20.

Synthesis of PLLA- or PDLA-Grafted Dextran. PLLA- or PDLA-grafted dextran (Dex-*g*-PLLA or Dex-*g*-PDLA) was synthesized through a coupling reaction between dextran and PLAs. In brief, dextran (200 mg, 5 μmol) and DMAP (110 mg, 920 μmol) were dissolved in dry DMSO (5 mL). Next, PLLA-CI or PDLA-CI (DP 20, 150 mg, 250 μmol) dissolved in dry DMSO (5 mL) was added. The solution was stirred at room temperature for 4 days in a nitrogen atmosphere, after which the reaction was stopped by addition of concentrated HCl (150 μL) to neutralize DMAP and imidazole. The reaction mixture was washed with a large amount of acetone to remove traces of uncoupled PLAs. The obtained precipitate was collected by centrifugation and dried under vacuum overnight to yield the white solid of Dex-*g*-PLLA or Dex-*g*-PDLA graft copolymers (DP = 20, average number of PLLA or PDLA chains per dextran molecule = 14).

Preparation of Aqueous Nanogel Solutions. Aqueous nanogel solutions were prepared by the solvent exchange method. Briefly, Dex-*g*-PLLA, Dex-*g*-PDLA, and an equimolar mixture of the two were first dissolved in DMSO, a solvent for both PLA and dextran. Subsequently, doubly distilled water was added to the copolymer/DMSO solutions at a rate of 1 drop every 10 s with vigorous stirring. The addition of water was continued until the water content reached 30−50 wt %, depending on the composition of the graft copolymers. The resulting solutions were transferred to dialysis tubes [molecular weight cutoff (MWCO) = 3500] and dialyzed against doubly distilled water to remove the organic solvent at room temperature. After dialysis, the solutions turned slightly opaque, except for G_1 and G_2 copolymers shown in Table 2, which exhibited transparent solutions. The samples for ^{1}H NMR and wide-angle X-ray diffraction (WAXRD) measurements were prepared by quick freezing in liquid nitrogen and thereafter lyophilized. The ^{1}H NMR spectra of the copolymer nanogels were obtained in DMSO-d_6 and D_2O separately at a concentration of 0.5 wt % to characterize the structure of the amphiphilic nanogels.

Measurement of Critical Aggregation Concentration. The critical aggregation concentrations (CAC) of Dex-*g*-PLLA, Dex-*g*-PDLA, and an equimolar mixture of the two in aqueous media were determined by use of pyrene as a fluorescence probe. Pyrene partitioned preferentially in the hydrophobic core of aggregates (nanogels) and changed the photophysical properties of the nanogels under investigation. Pyrene was first dissolved in acetone and then added to doubly distilled water to a concentration of 5×10^{-7} M. Acetone was subsequently removed by reducing the pressure and stirring for more than 5 h at 30 °C. The concentration of the copolymer in water was varied from 0.0001 to

Table 1. Characteristics of PLLA and PDLA[a]

polymer	M/OH	DP[b]	$M_{n,NMR}$[c]	$M_{n,GPC}$[d]	M_W/M_n[d]	yield (%)	$[\alpha]_D$[e] (deg)
PLLA(6)	6	6	910	930	1.52	82.5	−108
PDLA(6)	6	6	910	880	1.37	76.2	+102
PLLA(20)	22	20	2930	2720	1.61	80.7	−130
PDLA(20)	22	20	2930	2830	1.34	81.3	+127

[a] Ring-opening polymerization of lactide was carried out in THF for 10 min at room temperature. [b] Number of lactide units. [c] Estimated from ^{1}H NMR (solvent DMSO). [d] Estimated from GPC (eluent DMF, standard PS). [e] Values of optical rotation were measured at 20 °C with chloroform as the solvent, with a concentration equal to 10 mg/mL.

1.0 g/L. The pyrene and copolymer in the water were conjugated and equilibrated at room temperature for 1 day before measurement. The fluorescence spectra were measured at room temperature on a fluorescence spectrophotometer (Hitachi, F-2500). The emission spectrum of pyrene was obtained at a fixed excitation wavelength of 390 nm.

Dynamic Light Scattering Analysis on Dex-*g*-PLA Nanogels. Dynamic light scattering (DLS) measurement was carried out at 37 °C on a DLS-7000 apparatus (Otsuka Electronics Co.) with vertically polarized incident light with a wavelength of 488 nm supplied by an argon laser operated at 15 mW. Portions (15 mg) of Dex-*g*-PLLA, Dex-*g*-PDLA, and equimolar mixtures wweredissolved in 3.0 mL of doubly distilled water, and then the aqueous solutions were filtered through a Durapore (Millipore) 0.2 μm membrane prior to measurement.

Wide-Angle X-ray Diffraction Analysis on Dex-*g*-PLA Nanogels. The wide-angle X-ray diffraction patterns of the lyophilized samples were recorded on a M18XHF22-SRA instrument (MAC Science Co.) with Cu Kα source (λ = 1.54 Å) at 25 °C.

Atomic Force Microscopy on Dex-*g*-PLA Nanogels. Atomic force microscopy (SPA 400, soundproof housing, Seiko Instrument, Inc.) images of the nanogels were recorded in air at room temperature. These cantilevers have a resonance frequency around 110−150 kHz, a typical spring constant of about 15 N/m, and an integrated Si tip with a radius of curvature at the apex around 10 nm. The images were recorded in the intermittent-contact (tapping) mode. A volume of 5 μL of the nanogel solutions was dropped on a mica surface and air-dried for 1 h at room temperature prior to measurement.

Kinetic Stability Analysis of Dex-*g*-PLA Nanogels. Kinetic stability of the nanogels prepared from Dex-*g*-PLLA, Dex-*g*-PDLA, and equimolar mixtures was studied by DLS measurement in the presence of SDS, which acts as a destabilizing agent. The nanogel solutions (5.0 mg/mL) were mixed with an SDS aqueous solution (20 mg/mL) at a 2:1 (v/v) ratio, and the resulting mixed solutions were placed at 37 °C. After 2, 4, 6, 8, 10, 12, 24, 36, and 48 h, DLS measurements on the collapsing nanogels were performed at 37 °C.

Degradation Test of Dex-*g*-PLA Nanogels. To study the degradation behavior of the nanogels as a function of time, a cuvette was filled with 3.0 mL of the nanogel phosphate-buffered saline (PBS; pH = 7.4, I = 0.14) solutions and sealed with Parafilm to avoid contamination with dust particles. The cuvette was placed at 37 °C, and after 1, 2, 4, 6, 9, 12, 15, 18, 21, and 24 days, DLS measurements on the degrading nanogels were performed.

Results and Discussion

Synthesis of the Amphiphilic Dex-*g*-PLLA and Dex-*g*-PDLA Graft Copolymers. The synthesis of amphiphilic Dex-*g*-PLLA and Dex-*g*-PDLA graft copolymers was carried out through a two-step reaction. First, PLLA and PDLA were synthesized via ring-opening polymerization of L- AND D-lactide, respectively. The degree of polymerization (DP) of L- OR D-lactide was determined by integration ratio of the ^{1}H NMR (solvent DMSO-d_6) signals attributed to methyne proton of PLLA or PDLA at δ = 5.21 and methyl proton of ethanol at δ = 1.18. Characteristics of the obtained PLLA and PDLA are summarized in Table 1. Enantiomeric PLLA and PDLA with the same composition and high optical purity were obtained.

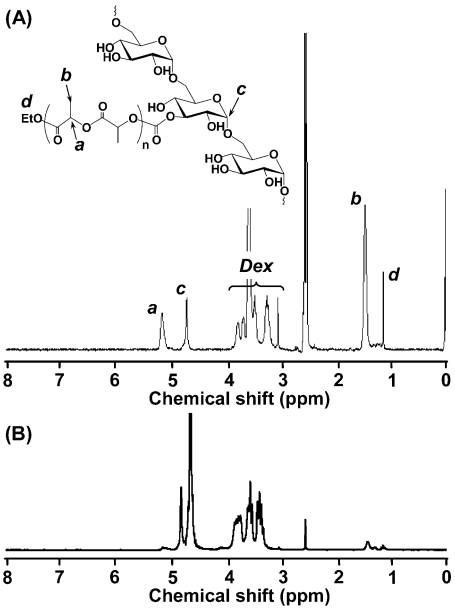

Figure 1. ^{1}H NMR spectra of G_7 copolymer (A) in DMSO-d_6 and (B) in D_2O at 37 °C.

After activation of hydroxyl end group with CDI, the resulting PLLA-CI and PDLA-CI were coupled to dextran to yield amphiphilic Dex-*g*-PLLA and Dex-*g*-PDLA graft copolymers, respectively. Size-exclusion chromatography (SEC) analysis demonstrated that no transesterification occurred under the selected reaction conditions. The average number of PLA chains per dextran molecule was calculated by integration ratio of the ^{1}H NMR (solvent DMSO-d_6) signals attributed to methyne proton of PLLA or PDLA at δ = 5.14 and anomeric proton of dextran at δ = 4.68−4.87, as shown in Figure 1. Absence of PLLA and PDLA uncoupled from the dextran backbone was confirmed by GPC measurement of the Dex-*g*-PLA copolymers (see Supporting Information). The characteristics of the obtained Dex-*g*-PLA copolymers were summarized in Table 2. The average number of PLA chains per dextran molecule for these copolymers ranged from 7 to 14. The contents of PLA in the copolymer were low, and the majority of the graft copolymers were dextran. Enantiomeric Dex-*g*-PLLA and Dex-*g*-PDLA copolymers with well-defined composition were obtained. Hydrophobic/hydrophilic balance of amphiphilic Dex-*g*-PLAs should affect the solubility in water. We found that the Dex-*g*-PLAs with high DP (40) of PLA grafts were not soluble in aqueous phase at all. Therefore, we chose relatively low DP (6 and 20) PLA grafts to obtain readily water-soluble Dex-*g*-PLA copolymers.

Formation of Dex-*g*-PLA Nanogels. To evidence the structure of the aggregates prepared from amphiphilic Dex-g-PLLA graft copolymer in dilute aqueous medium, the limited mobility of the PLLA chain in the core of the aggregates was explicated via ^{1}H NMR spectra in different solvent systems, DMSO-d_6 and D_2O. As presented in Figure 1A, the G_7

Table 2. Characteristics of Dex-*g*-PLLA and Dex-*g*-PDLA

code	copolymer	DP[a]	no. of PL(D)LA[b]	M_w/M_n[c]	$M_n \times 10^{-4}$	Dex content[d] (wt %)
G_1	Dex-*g*-PLLA(6-7)	6	7	1.86	4.64	86.2
G_2	Dex-*g*-PDLA(6-8)	6	8	1.90	4.73	84.6
G_3	Dex-*g*-PLLA(6-13)	6	13	2.08	5.18	77.2
G_4	Dex-*g*-PDLA(6-14)	6	14	2.03	5.27	75.6
G_5	Dex-*g*-PLLA(20-7)	20	7	2.12	6.05	66.2
G_6	Dex-*g*-PDLA(20-7)	20	7	1.88	6.05	66.2
G_7	Dex-*g*-PLLA(20-14)	20	14	1.95	8.10	49.6
G_8	Dex-*g*-PDLA(20-13)	20	13	2.01	7.81	51.2

[a] Number of lactide unit per PLA chain. [b] Average number of grafted PLA chains per dextran molecule by ^{1}H NMR (solvent: DMSO/D_2O = 8/1 v/v). [c] Determined by GPC (eluent: DMF, standard: PS). [d] Dextran unit content (wt %) = (M_n of original dextran/M_n of Dex-*g*-PLA) × 100.

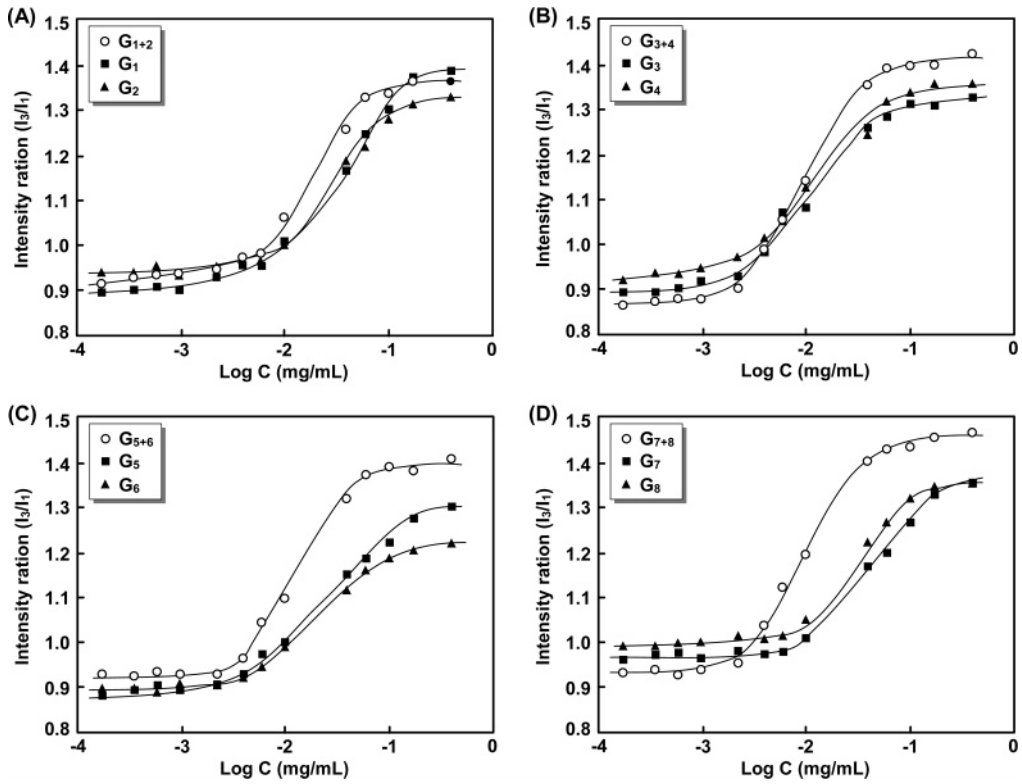

Figure 2. Plots of fluorescence intensity ratio I_{392}/I_{373} from pyrene excitation spectra vs log C for (A) G_1, G_2, and G_{1+2}; (B) G_3, G_4, and G_{3+4}; (C) G_5, G_6, and G_{5+6}; and (D) G_7, G_8, and G_{7+8} copolymers in water at 37 °C.

copolymer is dissolved in DMSO-d_6, where aggregate formation is not expected. Characteristic peaks of the methyl and methyne protons of PLLA were observed at 1.45 and 5.14 ppm, respectively. However, when the G_7 copolymer is dissolved in D_2O (Figure 1B), these peaks disappear, indicating that the PLLA segments form cores that cause a broadening effect, due to the restricted proton mobility of PLLA chains in ^{1}H NMR spectroscopy. On the other hand, characteristic peaks of the protons of the dextran, belonging to -CH or -CH_2 of the glycopyranose units, are in the range 3−5 ppm. Thus, these results suggests that the amphiphilic Dex-*g*-PLLA aggregates (nanogels) provide two domains consisting of the hydrophobic PLLA moiety and the hydrophilic dextran skeleton.[4] The same tendencies were observed in cases of Dex-*g*-PDLA copolymers as well as the equimolar mixtures between Dex-*g*-PLLA and Dex-*g*-PDLA copolymers with same composition. Accordingly, all Dex-*g*-PLA copolymers used in this study were confirmed to form nanogels in dilute aqueous solutions.

Critical Aggregation Concentration of Dex-*g*-PLA Copolymers in Aqueous Media. The formation of nanogels in dilute aqueous media and the critical aggregation concentration (CAC) for Dex-*g*-PLLA, Dex-*g*-PDLA, and equimolar mixtures were studied by the fluorescence technique with pyrene as a fluorescence probe. The partition of pyrene causes the emission peak shift from 373 (I_1) to 382 (I_3) nm (red shift), which means that PLA chains grafted on dextran start to form nanogels by intra- and/or intermolecular self-assembly of PLA in dilute aqueous solution. The transfer of pyrene from the polar environment to a nonpolar region significantly changes the intensity ratio of I_3/I_1 due to the increase in quantum yield of the fluorescence. As the concentration of the copolymer exceeds the CAC, the intensities of fluorescence increase substantially, suggesting the formation of nanogels. Figure 2 plots the intensity ratio (I_3/I_1) for the pyrene excitation spectra versus the logarithm of Dex-*g*-PLA concentration. The apparent CAC was obtained from the crossover point in the low-concentration range. The CAC values of graft copolymers with different compositions are listed in Table 3. All Dex-*g*-PLA copolymers exhibited low CAC values, and they were prone to decrease with increasing amounts of hydrophobic PLA. The CAC value of the equimolar mixtures of Dex-*g*-PLLA and Dex-*g*-PDLA copolymers (G_{1+2}, G_{3+4}, and G_{5+6}) is similar to that of the corresponding L- or D-isomers alone, except for G_{7+8} copolymer. Interestingly, the G_{7+8} copolymer only exhibited significantly lower CAC value

Table 3. Critical Aggregation Concentration[a] and Nanogel Size of Individual Copolymers and Mixed Aqueous Solutions[b]

code	copolymer	CAC (mg/L)	R_h[c] (nm)
G_1	Dex-*g*-PLLA(6-7)	7.3 ± 0.5	20.8
G_2	Dex-*g*-PDLA(6-8)	7.4 ± 0.7	18.4
G_{1+2}	Dex-*g*-PLLA(6-7) + Dex-*g*-PDLA(6-8)	6.8 ± 0.4	17.1
G_3	Dex-*g*-PLLA(6-13)	2.5 ± 0.5	16.1
G_4	Dex-*g*-PDLA(6-14)	2.7 ± 0.6	18.7
G_{3+4}	Dex-*g*-PLLA(6-13) + Dex-*g*-PDLA(6-14)	2.1 ± 0.2	16.6
G_5	Dex-*g*-PLLA(20-7)	4.1 ± 0.6	37.6
G_6	Dex-*g*-PDLA(20-7)	4.6 ± 0.8	40.3
G_{5+6}	Dex-*g*-PLLA(20-7) + Dex-*g*-PDLA(20-7)	4.3 ± 0.3	35.8
G_7	Dex-*g*-PLLA(20-14)	7.6 ± 0.6	47.3
G_8	Dex-*g*-PDLA(20-13)	8.0 ± 0.4	43.8
G_{7+8}	Dex-*g*-PLLA(20-14) + Dex-*g*-PDLA(20-13)	3.5 ± 0.6	72.6

[a] Critical aggregation concentration (CAC) was estimated by the fluorescent probe method. Mean of three independent experiments is shown. [b] Mixed aqueous solutions contained equimolar amounts of Dex-*g*-PLLA and Dex-*g*-PDLA copolymers in water at 37 °C. [c] Copolymer concentration 5.0 mg/mL. Measurements were performed at a scattering angle of 90° and a temperature of 37 °C.

compared with those of the G_7 and G_8 copolymers. The lower CAC values indicate a strong tendency of the Dex-*g*-PLA copolymers toward formation of stable nanogels. Additionally, PLA crystallites in the cores of G_{7+8} nanogels must be stabilized by strong van der Waals interactions. Thus, the results indicate that the G_{7+8} nanogels possess strong thermodynamic stability in aqueous solution and can perform as favorable drug carriers in our ongoing experiments on the drug loading characteristics.

DLS and Morphology Observation of Dex-*g*-PLA Nanogels. The hydrodynamic diameter (R_h) of nanogels was estimated by DLS measurement. Figure 3 shows the size and distribution of nanogels prepared from amphiphilic Dex-*g*-PLLA, Dex-*g*-PDLA, and equimolar mixtures. The aggregates exhibited nanometric sizes with R_h ranging from 16 to 73 nm (Table 3). The results indicate that the mean R_h of nanogels increases as the hydrophobic PLA chain length increase (e.g., G_1 and G_5), whereas there was no difference in R_h among the nanogels prepared from Dex-*g*-PLA copolymers with the same PLA chain length and different PLA numbers (e.g., G_1 and G_3). Thus, it will be possible to tune the nanogel size by varying the PLA chain length as well as the number of grafted PLA chains. For all these copolymers, relatively narrowly distributed nanogels were observed, indicating they were well-defined and presumably nanogels with hydrophobic PLA cores and hydrophilic dextran skeletons. The size and distribution of the mixed nanogels between equal amounts of the Dex-*g*-PLLA and Dex-*g*-PDLA copolymers with the same compositions (G_{1+2}, G_{3+4}, and G_{5+6}) were similar to those of the corresponding L- or D-isomers alone, except for G_{7+8} nanogel. Interestingly, the G_{7+8} copolymer exhibited significantly larger R_h and narrower distribution compared with those of the G_7 and G_8 copolymers.

Wide-Angle X-ray Diffraction Patterns of Dex-*g*-PLA Nanogels. In an attempt to gain insight into the physical state of the copolymer nanogel cores, wide-angle X-ray diffraction (WAXRD) studies of the lyophilized nanogel were carried out. Figure 4 shows the WAXRD patterns of the G_7, G_8, and G_{7+8} copolymer nanogels. There were no crystalline peaks in the case of G_7 and G_8 nanogels, indicating amorphous nature. Additionally, similar amorphous states were observed in case of the mixed nanogels between equal amounts of Dex-*g*-PLLA and Dex-*g*-PDLA copolymers (G_{1+2}, G_{3+4}, and G_{5+6}) (data not shown). On the contrary, G_{7+8} nanogels yielded crystalline peaks at 2θ values of 12.1° and 20.8°, which are characteristic of the

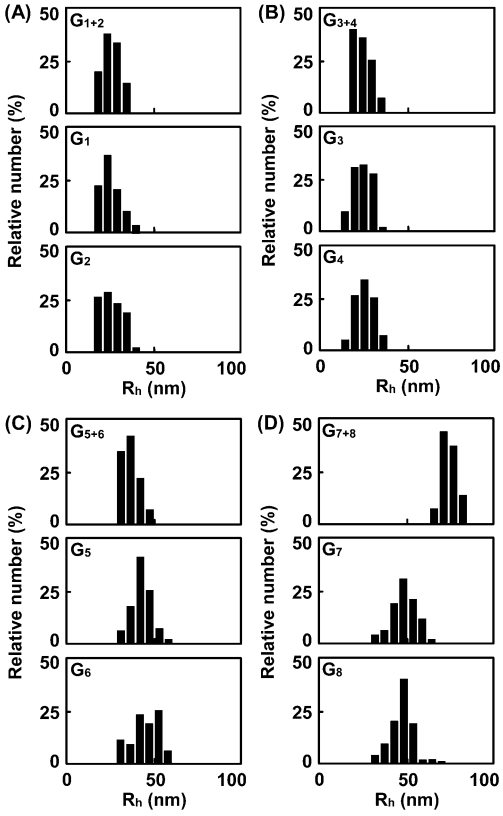

Figure 3. Size distribution for (A) G_1, G_2, and G_{1+2}; (B) G_3, G_4, and G_{3+4}; (C) G_5, G_6, and G_{5+6}; and (D) G_7, G_8, and G_{7+8} copolymer nanogels in water at 37 °C.

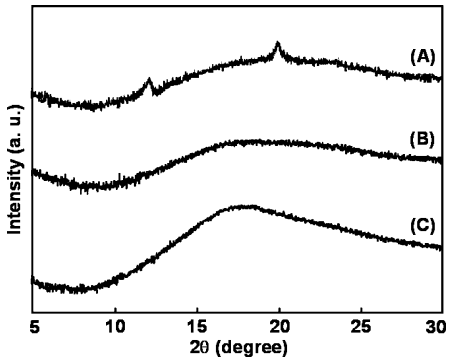

Figure 4. WAXRD patterns of (A) G_{7+8}, (B) G_7, and (C) G_8 copolymer nanogels.

crystalline structure of stereocomplex PLA. The results indicate that not only the DP of the PLA segment but also the number of grafted PLA chains is a key factor in determining the degree of stereocomplexation. Accordingly, it was concluded that significant thermodynamic stability as well as larger R_h and narrow distribution of the G_{7+8} nanogels was derived by stereocomplexation between grafted PLLA and PDLA chains in dilute aqueous solution. It is not clear, but the rearrangement of G_7 and G_8 copolymers by stereocomplexation will induce increased size and narrow distribution in G_{7+8} nanogel.

Morphology Observation of Dex-*g*-PLA Nanogels. Atomic force microscopy was used to visualize directly the size and morphology of the G_7, G_8, and G_{7+8} stereocomplex nanogels. Figure 5 demonstrates that the nanogels prepared from G_7 and G_8 copolymers were spherical with average diameters of 60 and 50 nm, respectively. The diameters of the nanogels shown in the AFM image are slightly larger than those obtained from DLS measurements, perhaps because the nanogels adsorbed onto

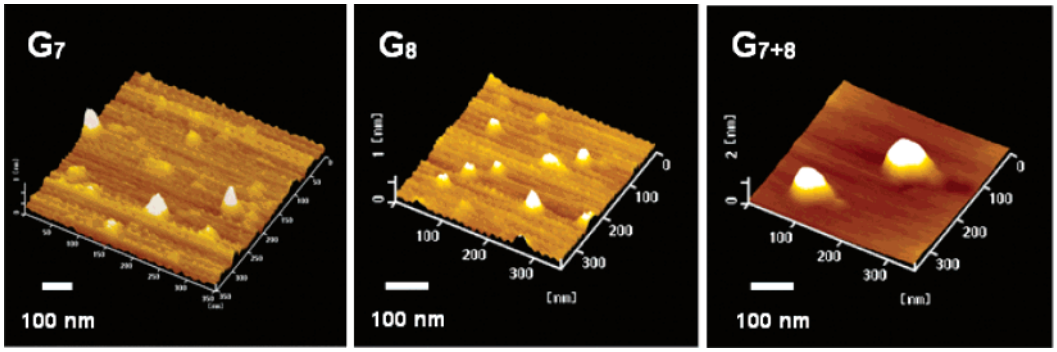

Figure 5. AFM images of the G_7, G_8, and G_{7+8} copolymer nanogels. Imaging was performed in air on a mica surface and in tapping mode by use of an etched silicon tip.

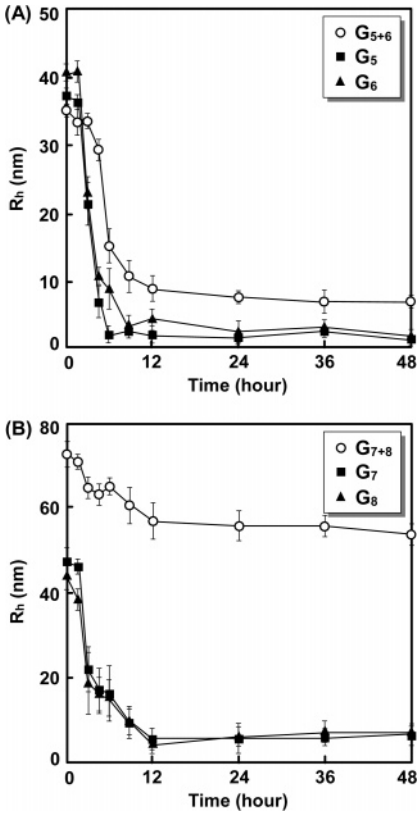

Figure 6. Hydrodynamic diameter (R_h) of (A) G_5, G_6, and G_{5+6} and (B) G_7, G_8, and G_{7+8} copolymer nanogels vs time after addition of SDS (6.7 mg/mL final concentration) at 37 °C. Mean ± SD of three independent experiments is shown.

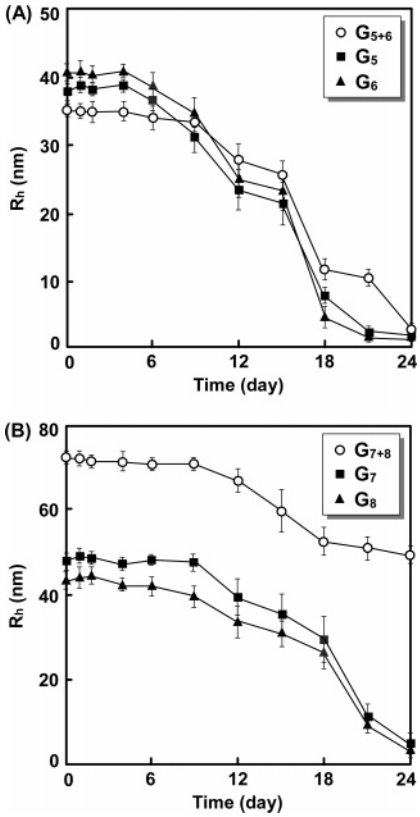

Figure 7. Hydrodynamic diameter (R_h) of (A) G_5, G_6, and G_{5+6} and (B) G_7, G_8, and G_{7+8} copolymer nanogels vs time after incubation in PBS at 37 °C. Mean ± SD of three independent experiments is shown.

mica surface slightly spread during the drying procedure. It can be seen that the G_{7+8} stereocomplex nanogel most often has a spherical shape with average diameter 90 nm and a size close to that measured by DLS. Additionally, AFM images confirmed the narrow size distribution of G_{7+8} stereocomplex nanogel.

Kinetic Stability of Dex-*g*-PLA Nanogels. Kinetic stability of the nanogels prepared from Dex-*g*-PLLA, Dex-*g*-PDLA, and equimolar mixtures was studied by DLS measurement in the presence of SDS, which acts as a destabilizing agent. Figure 6 shows the time dependence in mean R_h of amorphous G_{5+6} and G_{7+8} stereocomplex nanogel systems with different numbers of grafted PLA chains. SDS-treated G_{5+6} nanogel system with amorphous PLA cores exhibited a drastic decrease in R_h to about 3 nm within 10 h, suggesting the complete dissociation of nanogels by addition of SDS. Similar trends were also observed but to a smaller extent with G_7 and G_8 nanogels, suggesting the dissociation of a large fraction of nanogels. Stability could be slightly improved by increasing the number of grafted PLA chains up to 14. On the other hand, G_{7+8} stereocomplex nanogel was substantially more stable as it showed only a minimal decrease in mean R_h. Even after 2 days, the G_{7+8} stereocomplex nanogel retained more than 75% of its initial R_h, indicating strong kinetic stability in dilute aqueous solution. Thus, G_{7+8} stereocomplex nanogel can be expected to show an advantage for requirements such as long circulation times, accumulation at targeted sites, and as the vehicles of bioactive agents.

Degradation Behavior of Dex-*g*-PLA Nanogels. Degradation behavior of the nanogels prepared from Dex-*g*-PLLA, Dex-*g*-PDLA, and equimolar mixtures was studied by DLS measurement in PBS at 37 °C. Figure 7 shows the time dependence in mean R_h of amorphous G_{5+6} and G_{7+8} stereocomplex nanogel systems with different numbers of grafted PLA chains. Clearly, the R_h of all the nanogels decreased, indicating that they indeed degrade. Considering the gradual decrease in R_h of these nanogels at early stage, at a first sight one could argue that the nanogels degrade through erosion of water-soluble degraded

oligolactide. On the other hand, the drastic decrease in R_h of G_{5+6} nanogel system at late stage suggests the complete dissociation of nanogels due to collapse of the degraded PLA cores. Similar trends were also observed but to a smaller extent with G_7 and G_8 nanogels, suggesting a slower degradation rate. In contrast, G_{7+8} stereocomplex nanogel exhibited a substantially slower degradation rate as it showed only a minimal decrease in mean R_h. Even after 24 days, the G_{7+8} stereocomplex nanogel retained more than 60% of its initial R_h, indicating relative stability of the PLA stereocomplex cores in nanogels against hydrolysis. These results imply that the degradation behavior of Dex-*g*-PLA nanogels is tunable not only by varying the number of grafted PLA chains but also by applying stereocomplexation. The gradual and tunable degradation behavior could be of interest to regulate drug release from the Dex-*g*-PLA nanogels after uptake by cells.

Conclusions

In this study, amphiphilic graft copolymers with a backbone of dextran and enantiomeric side chains of PLLA or PDLA were prepared. Enantiomeric Dex-*g*-PLLA and Dex-*g*-PDLA copolymers with well-defined composition were obtained through the coupling reaction between dextran and PLA. ^{1}H NMR in D_2O provided evidence of aggregate formation with two domains consisting of the hydrophobic PLA cores and the hydrophilic dextran skeleton by intra- and/or intermolecular self-assembly of PLA chains in a dilute aqueous solution. All Dex-*g*-PLA copolymers exhibited low CAC values, and they were prone to decrease with increasing amounts of hydrophobic PLA. The CAC values of the equimolar mixtures of the L- or D-isomers (G_{1+2}, G_{3+4}, and G_{5+6}) is similar to that of the corresponding L- or D-isomers alone, except for the G_{7+8} copolymer. Interestingly, the G_{7+8} copolymer exhibited a significantly lower CAC value compared with that of the G_7 and G_8 copolymers, indicating high ability of G_{7+8} copolymer to form aggregates and strong thermodynamic stability. The mean diameters of the aggregates ranged from 16 to 73 nm with narrow size distribution, indicating they were well-defined and presumably nanogels. Furthermore, only G_{7+8} nanogel exhibited substantially strong kinetic stability as it showed only a minimal decrease in mean diameter upon addition of SDS, which acts as a destabilizing agent. There were no crystalline peaks in WAXRD patterns of the G_{1+2}, G_{3+4}, and G_{5+6} nanogels, whereas G_{7+8} nanogels yielded crystalline peaks at 2θ values of 12.1° and 20.8°, indicating the stereocomplexation of PLA. So we found that stereocomplex crystallites were formed in the case of Dex-*g*-PLA copolymers having both adequate DP and a relatively large number of PLA grafts. In other words, both the DP and the number of PLA grafts are key factors to determine the degree of stereocomplexation in case of water-soluble Dex-g-PLA copolymers in dilute aqueous media. Accordingly, it was concluded that the strong thermodynamic as well as kinetic stabilities of the G_{7+8} nanogels were derived by stereocomplexation. The results of the degradation test suggest that the degradation behavior of Dex-*g*-PLA nanogels is tunable not only by varying the number of grafted PLA chains but also by applying stereocomplexation. Namely, G_{7+8} stereocomplex nanogel can be expected to show an advantages requirements such as long circulation times, accumulation at targeted sites, and controlled drug release as the vehicles of bioactive agents.

Acknowledgment. This work was carried out as a study in the High-Tech Research Center Project supported by the Ministry of Education, Culture, Sports, Science and Technology, Japan.

Supporting Information Available. GPC profiles of G_5, dextran, and PLLA(20). This material is available free of charge via the Internet at http://pubs.acs.org.

References and Notes

(1) Zhang, L.; Eisenberg, A. *Science* **1995**, *268*, 1728−1731.
(2) Cornelissen, J. J. L. M.; Fischer, M.; Sommerdijk, N. A. J. M.; Nolte, R. J. M. *Science* **1998**, *280*, 1427−1430.
(3) Bellomo, E. G.; Wyrsta, M. D.; Pakstis, L.; Pochan, D. J.; Deming, T. J. *Nat. Mater.* **2004**, *3*, 244−248.
(4) Akiyoshi, K.; Deguchi, S.; Moriguchi, N.; Yamaguchi, S.; Sunamoto, J. *Macromolecules* **1993**, *26*, 3062−3068.
(5) Morimoto, N.; Endo, T.; Iwasaki, Y.; Akiyoshi, K. *Biomacromolecules* **2005**, *6*, 1829−1834.
(6) Kadlubowski, S.; Grobelny, J.; Olejniczak, W.; Cichomski, M.; Ulanski, P. *Macromolecules* **2003**, *36*, 2484−2492.
(7) Van Thienen, T. G.; Lucas, B.; Flesch, F. M.; Nostrum, C. F.; Demeester, J.; De Smedt, S. C. *Macromolecules* **2005**, *38*, 8503−8511.
(8) Lee, W. C.; Li, Y. C.; Chu, I. M. *Macromol. Biosci.* **2006**, *6*, 846−854.
(9) Yan, M.; Ge, J.; Liu, Z.; Ouyang, P. *J. Am. Chem. Soc.* **2006**, *128*, 11008−11009.
(10) Rodrigues, J. S.; Santos-Magalhaes, N. S.; Coelho, L. C. B. B.; Couvreur, P.; Ponchel, G.; Gref, R. *J. Controlled Release* **2003**, *92*, 103−112.
(11) Kakizawa, Y.; Harada, A.; Kataoka, K. *J. Am. Chem. Soc.* **1999**, *121*, 11247−11248.
(12) Ma, Q.; Remsen, E. E.; Kowalewski, T.; Schaefer, J.; Wooley, K. L. *Nano Lett.* **2001**, *1*, 651−655.
(13) Kricheldorf, H. R.; Kreiser-Sanders, I. *Macromol. Symp.* **1996**, *103*, 85−102.
(14) Ogawa, Y.; Yamamoto, M.; Ogawa, H.; Yashiki, T.; Shimamoto, T. *Chem. Pharm. Bull.* **1988**, *36*, 1095−1103.
(15) Langer, R.; Vacanti, P. *Science* **1993**, *260*, 920−926.
(16) Slager, J.; Domb, A. J. *Adv. Drug Delivery Rev.* **2003**, *55*, 549−583.
(17) Ikada, Y.; Jamshidi, K; Tsuji, H.; Hyon, S. H. *Macromolecules* **1987**, *20*, 906−908.
(18) Kang, N.; Perron, M. E.; Prud'homme, R. E.; Zhang, Y.; Gaucher, G.; Leroux, J. C. *Nano Lett.* **2005**, *5*, 315−319.
(19) De Jong, S. J.; De Smedt, S. C.; Wahls, M. W. C.; Demeester, J.; Kettenesvan, B. J. J; Hennink W. E. *Macromolecules* **2000**, *33*, 3680−3686.
(20) Lim, D. W.; Choi, S. H.; Park T. G. *Macromol. Rapid Commun.* **2000**, *21*, 464−471.
(21) Slivniak, R.; Domb, A. J. *Biomacromolecules* **2002**, *3*, 754−760.
(22) Li, S. M.; Vert, M. *Macromolecules* **2003**, *36*, 8008−8014.
(23) Mukose, T.; Fujiwara, T.; Nakano, J.; Taniguchi, I.; Miyamoto, M.; Kimura, Y.; Teraoka, I.; Lee C. W. *Macromol. Biosci.* **2004**, *4*, 361−367.
(24) Hiemstra, C.; Zhong, Z.; Li, L.; Dijkstra, P. J.; Feijen, J. *Biomacromolecules* **2006**, *7*, 2790−2795.
(25) Cai, Q.; Wan, Y.; Bei, J.; Wang, S. *Biomaterials* **2003**, *24*, 3555−3562.
(26) Nouvel, C.; Frochot, C.; Sadtler, V.; Dubois, P.; Dellacherie, E.; Six, J. L. *Macromolecules* **2004**, *37*, 4981−4988.
(27) Thanki, P. N.; Dellacherie, E.; Six, J. L. *Eur. Polym. J.* **2005**, *41*, 1546−1553.
(28) Ouchi, T.; Kontani, T.; Ohya, Y. *Polymer* **2003**, *44*, 3927−3933.
(29) Ouchi, T.; Kontani, T.; Saito, T.; Ohya, Y. *J. Biomater. Sci., Polym. Ed.* **2005**, *16*, 1035−1045.

BM070206T